



SPECIAL ISSUE: Excitonic Solar Cells (I)

Impact of sol aging on TiO₂ compact layer and photovoltaic performance of perovskite solar cell

Lixue Guo¹, Chengbin Fei¹, Rong Zhang¹, Bo Li², Ting Shen², Jianjun Tian^{1,2*} and Guozhong Cao^{1,3*}

ABSTRACT Perovskite solar cells are known to have a power conversion efficiency dependent on subtle variation in chemical composition and crystal and microstructures of materials, processing conditions, and device fabrication procedures and conditions. The present work demonstrates such strong dependence of power conversion efficiency on a TiO₂ film made of the same sol with various aging time. A dense and conformal TiO₂ film was prepared by sol-gel method, and the influences of its surface morphology and thickness on performance of perovskite solar cells have been investigated. The surface morphology and thickness of the TiO₂ film were tuned by adjusting the aging time of sol, resulting in enhanced short-circuit current density and fill factor of the perovskite solar cells due to increased coverage and roughness of perovskite films, light refraction, and effective charge recombination blocking effect, which were verified by means of the light absorption spectra, photoluminescence of perovskite films with and without hole transport layer, cyclic voltammogram, and electrochemical impedance spectra. The cells with a dense and conformal TiO₂ compact layer derived from the sol aged for 4 h exhibit a power conversion efficiency of 15.7%, 50% higher than the efficiency based on TiO₂ layer derived from 0 h aging sol and 3 times of the efficiency with TiO₂ layer made from 8 h aged sol.

Keywords: perovskite solar cells, TiO₂ sol, compact layer, aging time

INTRODUCTION

Titanium oxide (TiO₂), as a classical n-type semiconducting oxide has three crystal forms: brookite, rutile and anatase [1]. The anatase TiO₂ with a band gap of 3.2 eV has found wide applications, such as photocatalysis, chemical and bio-sensors and photovoltaics [2–5]. TiO₂ thin films

are often used as photoanode in new generation thin film solar cells, such as dye-sensitized solar cell [6], perovskite solar cell [7] and quantum dot solar cell [8]. Nowadays the thin film solar cells based on organolead halide perovskite (CH₃NH₃PbI₃) have attracted a lot of interest and enthusiasm due to their higher absorption coefficient, long carrier diffusion length, suitable band gap (about 1.5 eV) and high electronic qualities [9–13]. The cell structure has been extended from solid-state perovskite-sensitized solar cell to planar heterojunction solar cell [14–16]. In planar heterojunction structure, the perovskite film also serves as electron transport other than only absorbing material in the sensitized structure [17,18]. The schematic illustration of the cell structure is shown in Fig. 1. TiO₂ dense film is used as the compact layer which plays an important role in charge transfer. It can effectively prevent charge recombination at the interface of fluorine-doped tin dioxide (FTO) and perovskite or hole transport material (HTM) layer [19–21]. Additionally, the compact layer can reduce energy barrier between FTO and the active layer, which benefits charge extraction. Furthermore, the band gap of TiO₂ is around 3.2 eV (corresponding to the absorption edge of about 380 nm), so the compact layer can protect perovskite layer by absorbing UV-light. Therefore, the desired quality of the compact layer has great positive effects on solar cell performance.

The properties of TiO₂ compact films vary with prepared methods, doping with other elements and surface treatments [21–23]. It has been demonstrated that the thickness, morphology and surface condition of the compact layer can affect the power conversion efficiency (PCE) of

¹ Beijing Institute of Nanoenergy and Nanosystems, Chinese Academy of Sciences; National Center for Nanoscience and Technology (NCNST), Beijing 100083, China

² Advanced Material and Technology Institute, University of Science and Technology, Beijing 100083, China

³ Department of Materials and Engineering, University of Washington, Seattle, Washington 98195-2120, USA

* Corresponding authors (emails: gzc@u.washington.edu (Cao G), tianjianjun@mater.ustb.edu.cn (Tian J))

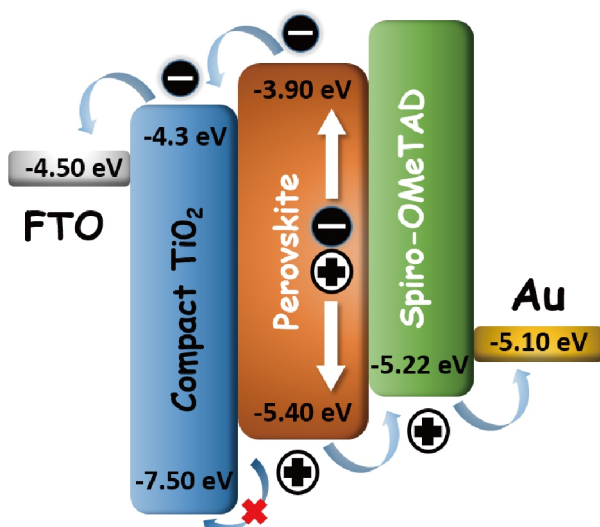


Figure 1 Schematic illustration of energy levels of the cell and blocking effect of the compact layer.

solar cells, whereas the compactness is a key character. This research reports a systematic experimental study about effects of surface condition and thickness of the sol-gel derived TiO_2 films on its compactness and further on the performances of perovskite solar cells primarily through the control of sol aging. The TiO_2 films with different surface condition and thickness varying from 50 to 170 nm were prepared by adjusting sol aging time from 0 to 8 h. The surface condition of the films was investigated by scanning electron microscopy (SEM) and atomic force microscopy (AFM). And the compactness was verified by cyclic voltammogram (CV) measurement and electrochemical impedance spectra (EIS). The photoluminescence of the perovskite films deposited on different TiO_2 compact layer with and without hole transport layer was also studied to reveal the impacts of TiO_2 compact layer on perovskite film and its charge injection. The final performance enhancement is likely resulted from both increased short-circuit current density (J_{sc}) and fill factor (FF).

EXPERIMENTAL SECTION

Preparation of the TiO_2 compact layers

The TiO_2 sol was prepared by a modified sol-gel process which was originally described in literature [24]. Firstly, 0.13 mmol of titanium tetra isopropoxide (Aladdin, 99.999%) was added into 2.5 mL of anhydrous ethanol in a 10-mL volumetric flask. Then hydrochloric acid (HCl, 2 mol L^{-1}) as control agent was added dropwise (pH 1.5,

about 40 μL). After vigorously stirring, the solution was poured into a 10-mL beaker and stood for hydrolytic condensation occurrence at room temperature. At different stages of aging process, a series of compact film samples were prepared by spin coating the sols aged for 0, 2, 4, 6 and 8 h at 2000 rpm.

Precursor preparation

Methylamine iodide (MAI) was prepared by a previously reported method [25,26]. Methylamine in methanol (33 wt.%) was mixed with hydroiodic acid (HI, 57 wt.%) in a molar ratio of 1.2:1 at 0°C . The HI was added dropwise while stirring. After stirring for 2 h, the solvent was removed through evaporation using rotary evaporator at 60°C . Then the obtained powder was washed by diethyl ether, and re-crystallized in methanol at room temperature. Finally, the white powder was dried at 60°C for 24 h in vacuum oven. As for the methylamine chloride (MACl), hydroiodic acid was replaced by hydrochloric acid (HCl, 33 wt.%). The other procedure was all the same with that of MAI.

The perovskite precursor was prepared by dissolving PbI_2 , MAI, and MACl in *N,N*-dimethylformamide (DMF) at a 1:1:1 molar ratio, and stirred at 70°C for 3 h, with final concentration of 0.52 mol L^{-1} [27]. The hole-transporting layer precursor was a solution of 1 mL chlorobenzene with 72.3 mg spiro-OMeTAD, 28.8 μL 4-tert-butylpyridine and 17.5 μL of a 170 mg mL^{-1} bis(trifluoromethane)sulfonimide lithium salt (LiTFSI).

Fabrication of solar cells

The substrate of solar cells was FTO coated glass. Initially, the FTO was etched by zinc powder and HCl (2 mmol L^{-1}), and the glasses were cleaned with deionized water, acetone, deionized water, ethanol and oxygen plasma. Then a TiO_2 blocking layer was deposited by spin coating the prepared precursor which was aged for different time, at 2000 rpm for 30 s, and sintered at 500°C for 30 min (rate: $10^\circ\text{C min}^{-1}$). The perovskite precursor was spin-coated on the compact layer, at 2000 rpm for 20 s and dried at 100°C for 1.5 h with both the substrates and precursor pre-heated at 70°C . When the samples were cooled down, a hole-transporting layer was deposited via spin coating at 4000 rpm for 30 s. The devices were allowed to oxidize overnight in a desiccator, and finally, a gold layer was deposited by thermal evaporation.

Characterization

The SEM measurements were performed using a field emission scanning electron microscope (SU8020, Hitachi Co.). The AFM measurements were undertaken by using

an Asylum Research (MEP-3D-SA) operated in trapping mode. The absorption spectra were recorded using a Shi-madzu (UV-3600) UV-vis spectrophotometer ranging from 300 to 900 nm. The photoluminescence (PL) measurements were taken by using a Horiba scientific Fluorolog spectrometer and a green laser (532 nm) was used as excitation source. The current density-voltage (J - V) curves were measured under AM 1.5 simulated sunlight (Oriel Sol 3A Solar Simulator, 94063A, Newport Stratford Inc.), equipped with a 300 W Xenon lamp (Newport) and was recorded by a electrochemical workstation (Zahner Company, Germany). The irradiation intensity was calibrated to 100 mW cm^{-2} with a standard reference crys-

talline silicon solar cell (Stratford Inc., 91150 V, Newport). The EIS measurements were recorded by IM6ex (Zahner Company, Germany), using light emitting diodes ($\lambda = 455 \text{ nm}$) driven by Expot (Zahner Company, Germany).

RESULTS AND DISCUSSION

The surface morphology and thickness of the compact layers prepared by sols aged for different period of time were observed by SEM and AFM (Fig. 2). As described in experimental section, all the films were spin coated on FTO substrate, followed by annealing at 500°C for 30 min in air that were all under the same procedure and identical processing conditions. Fig. 2 shows that the thickness of the

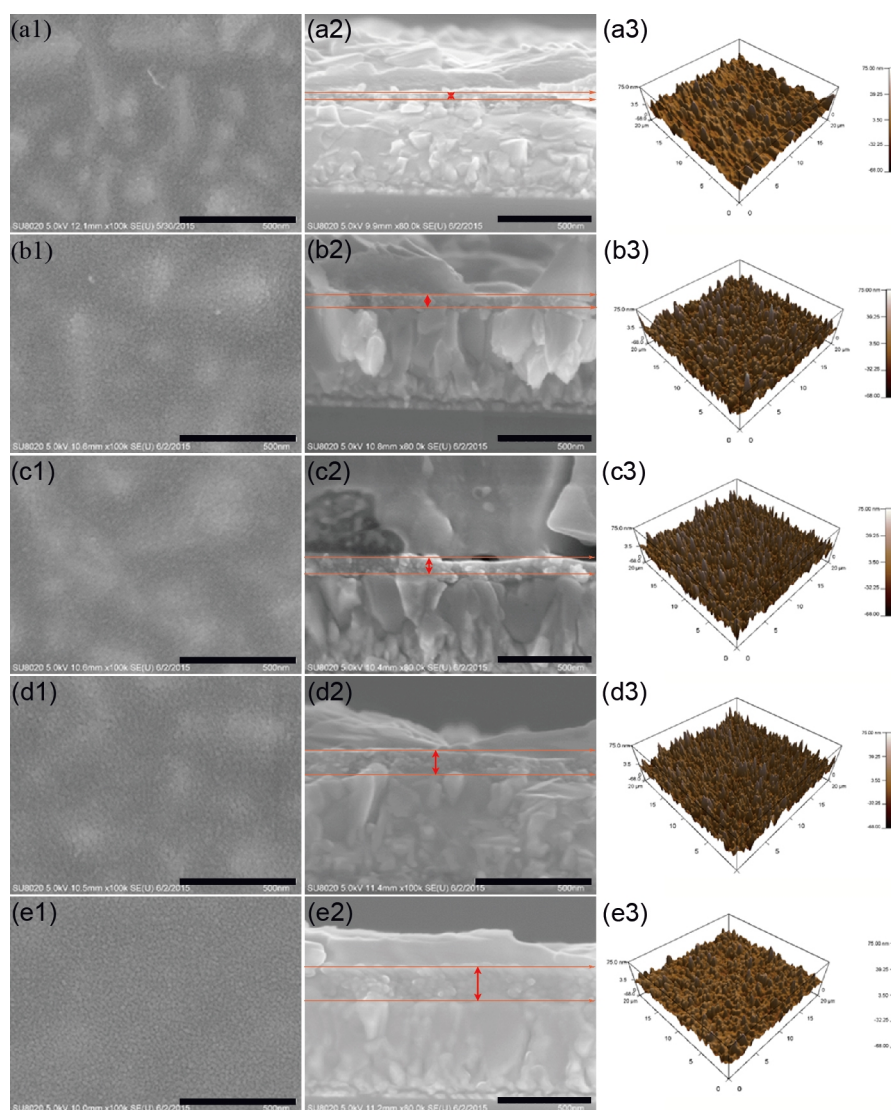


Figure 2 SEM images showing the surface morphology (on the left side), the cross-section (in the middle column) and the AFM images (on the right side) of TiO_2 compact layers made by sols with different aging time: (a) no aging (0 h), (b) aged for 2 h, (c) aged for 4 h, (d) aged for 6 h, and (e) aged for 8 h.

films increases monotonically from 42 to 170 nm and the particle size in films increases from several nanometers to around 55 nm, as the sol aging time increases from 0 to 8 h. The ultrathin films derived from 0 and 2 h aged sols may have not formed full coverage on the FTO surface. When the aging time increases to 4 h, a conformal film is likely obtained, which still reflects the morphology of FTO surface beneath the TiO₂ coating. Further increase of aging time to 8 h results in further increase of the thickness with cracking (Fig. S1). The surface roughness of the TiO₂ films analyzed from AFM measurements increases first and then decreases with prolonged sol aging time as summarized in Table 1. The film made from 4 h aged sol has the largest roughness, as a result of combining the roughness of TiO₂ compact layer and FTO substrate surface morphology. When the aging time is short, a thin TiO₂ coating may not cover the entire FTO surface to form a complete coverage; instead it may recede to the concave surface pockets resulting in a reduced surface roughness. Although an excessive aging results in more extended condensation of TiO₂ clusters, the resultant thick coating would eliminate or shadow the rough morphology of the underneath FTO surface, and thus lead to a reduced surface roughness as well. Further investigation is underway to verify the above proposed explanation.

Fig. 3 illustrates a possible formation process of sol aging and the corresponding compact layers. The process involves the conversion of monomers into a colloidal dispersion (sol) through multistep and reversible hydrolysis and condensation reactions; the monomers incorporate to the existing nanoclusters (or colloidal particles) and the monoclusters connect with each other through condensation reactions during sol aging, resulting in growth of nanoclusters/nanoparticles [28]. If the sol is allowed to age sufficiently, those nanoclusters would eventually form a percolated network, known as sol-gel transition or gelation. The thickness of film is determined by the concentration of the solid content, the viscosity, and spinning speed. With aging time increases, both particle size and viscosity of the sol would increase in theory. In practice, the viscosity would have no detectable increase until reaching the sol to gel transition, at which the viscosity increases drastically and exponentially converting the liquid sol to solid gel [29]. Similarly the particle size would change little during aging. However, aging would allow the condensation process to proceed continuously with the individual particles/clusters to connect with one another and with the aggregated particles/clusters to grow as schematically indicated in Fig. 2. Since the particles or clusters or aggregates are significantly small, their size monitoring or determination remains dif-

Table 1 Sample parameters of the TiO₂ compact layers deposited by spin coating the sols aged for different duration: 0, 2, 4, 6 and 8 h

Samples	Roughness (nm)	Thickness (nm)	Peak gap (V)	Recombination resistance (kΩ)
0 h	7.01	42	/	/
2 h	10.92	62	1.229	2.00
4 h	11.27	75	1.531	2.95
6 h	9.84	100	1.375	1.72
8 h	6.88	170	/	/

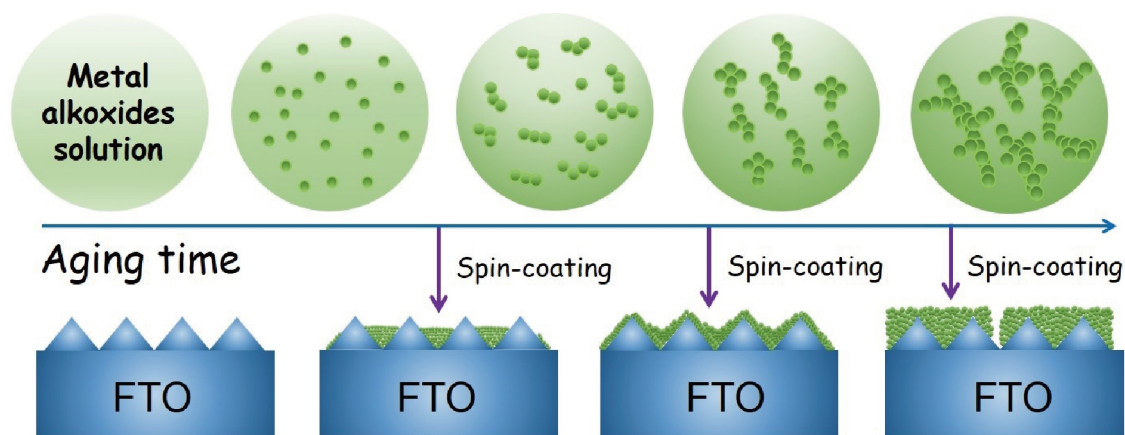


Figure 3 The scheme illustration of aging process in the sol and the corresponding TiO₂ compact films.

difficult at this moment. Although the quantum confinement has been widely and successfully used to determine the size change of quantum dots of narrow bandgap semiconductors [30], the quantum confinement in wide bandgap semiconductors like TiO_2 studied in this work is very difficult to achieve. Yet another method using the Scherer equation to calculate the crystallite size from the corresponding XRD patterns has been widely accepted for the characterization of commonly well crystallized samples; however, the sol-gel derived TiO_2 films prior to thermal annealing have very poor crystallinity (Fig. S2).

The morphological difference in compact film will affect the crystallinity and physical properties of the perovskite film subsequently deposited on the top of it. Fig. 4 shows the UV-vis absorption spectra of the perovskite films deposited on different compact layers. It is found that the perovskite film deposited on compact layers derived by sol aged for 4 h has the best absorption. This may be due to two possible reasons: one is that the biggest roughness of 4 h compact layers leads to better coverage and thickest perovskite film, resulting in best light absorption and the other is that the biggest roughness results in strongest scattering with much increased light travel distance within the perovskite film benefiting the absorption. Light absorption is the first step of photo-to-electric energy conversion in a solar cell, which determines the J_{sc} .

The TiO_2 dense films in solar cells are to block hole transport, so compactness is the primary property of compact layer. The blocking effect of the compact TiO_2 films toward charge transfer across the FTO (TiO_2)/electrolyte interface is assessed by CVs. The CV measurements were performed

in aqueous electrolyte containing I_3^-/I^- as probing redox. Because the dense TiO_2 films block the access of redox probe to FTO, the compactness of the TiO_2 films can be monitored. In the CVs, the separation voltage between oxidation and reduction peaks directly reflects the difficulty of charge recombination [31,22]. Fig. 5 compares the CVs and shows the separation voltage varying appreciably with different compact layers, and the separation voltages are summarized in Table 1. Without TiO_2 compact layer, the separation voltage is the smallest, ~ 1.1 V and the peak current density for both oxidation and reduction peaks is the largest, ~ 0.63 mA cm^{-2} revealing the easy charge transfer (or charge recombination). When a TiO_2 compact layer is applied, the separation voltage increases appreciably and the peak current density decreases, indicative of the effectiveness of blocking charge transfer or charge recombination. The separation voltage increases first from 1.07 to 1.27 V, when the aging time increases from 2 to 4 h; however, the further increase of the aging time to 6 h results in a decreased separation voltage to 1.17 V, likely due to the existence of cracks formed in the thick TiO_2 films. The CV results are further compared with and supported by the EIS data as discussed below.

The EIS measurements were conducted on the complete solar cell devices with different compact layers to verify its impacts on charge transfer and transport properties. In a typical Nyquist plot of perovskite solar cell, the high frequency arc is commonly associated with the hole transport in HTM, while the arc at lower frequencies is related to recombination resistance at the interface [32]. Fig. 6 shows the Nyquist plots of the devices with different compact lay-

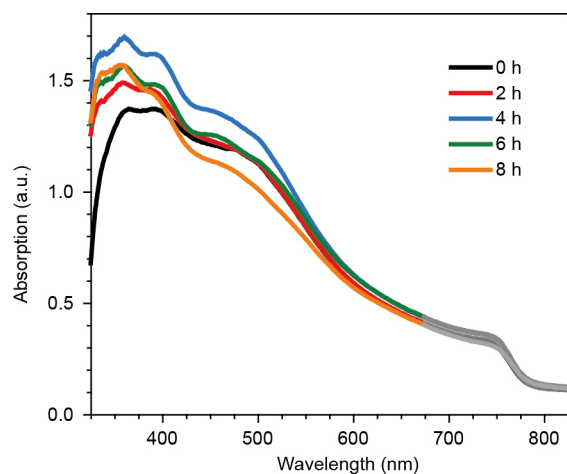


Figure 4 The UV-vis absorption spectra of the perovskite films deposited on TiO_2 films made from sols aged for various durations: 0, 2, 4, 6 and 8 h.

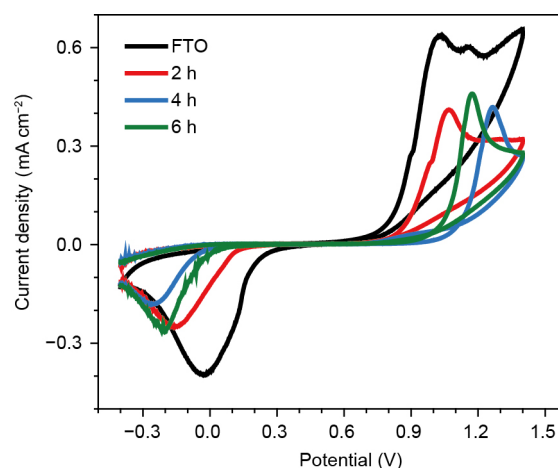


Figure 5 The CV curves of bare FTO and FTO with spin-coated TiO_2 compact layers made from sols aged for 2, 4 and 6 h, respectively, using the I_3^-/I^- as probing redox, scan velocity: 50 mV s^{-1} , potential vs. Ag/AgCl .

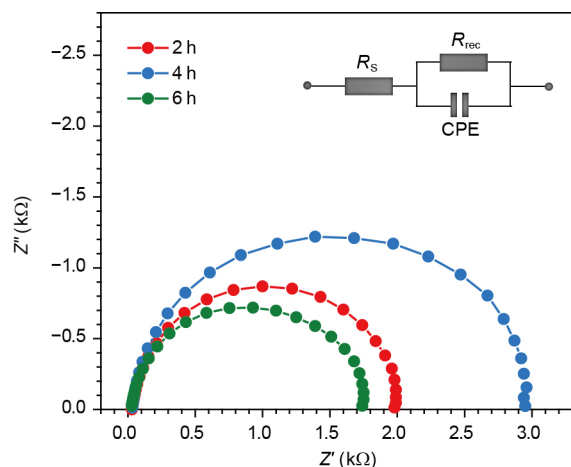


Figure 6 The Nyquist plots from the EIS of perovskite solar cells with compact layers made from sols aged for 2, 4 and 6 h at a bias potential of 0.8 V in dark. The proposed equivalent circuit is included.

ers, as measured with a bias potential of 0.8 V in dark. The Nyquist plots are clearly dominated by the semicircle at intermediate frequency, which is related to the recombination resistance of cell. Therefore, a relatively simple equivalent circuit has fitted to the data (the inset) [33,34]. The presumed small semicircle in the high frequency region is not found, indicating very small transport resistance in HTM. Diameter of the semicircle represents the recombination resistance which is summarized in Table 1. The cell with a TiO₂ compact layer made by sol aged for 4 h has the biggest recombination resistance, which resulted from the most reduced charge recombination. The reduction of charge recombination would enhance both the J_{sc} and FF of

the solar cells when other parameters remain the same.

The PL measurements were executed to study the excitation dissociation and charge transport [16,35]. Two types of structures with compact layers made from the sols aged for 2, 4, and 6 h were made and subjected to PL measurements. The structure of the first set of samples is FTO/compact layer/perovskite layer (the inset). As shown in Fig. 7a, the samples just have one light absorption function, so photo-generated electron-hole pairs would not be easily separated and transported away or dispersed effectively if the compact layer functions well [36]. The higher PL emission of the perovskite film deposited on 4 h compact film is indicative of better blocking character of compact layer, than both the TiO₂ films aged for 2 or 6 h. The second set of structures is with the addition of HTM layers on the perovskite films, so a p-n junction is formed in each sample. Therefore, photo-generated electron-hole pairs can be readily dissociated and dispersed, resulting in serious luminescence quenching. The PL presented in Fig. 7b, has a similar intensity as that in Fig. 7a., even though the laser intensity applied here is 2 orders of magnitude stronger than that used for the first samples, due to the significant quenching effect. Comparison of the PL in Fig. 7b reveals that the samples with compact films made by sol aged for 4 h show the most obvious quenching effect, indicating that the exciton separation and transfer is most effective [37]. The biggest roughness of the TiO₂ film from 4 h aged sol may provide the best contact between the TiO₂ and perovskite film and offer the most effective electron transfer, and consequently reduce charge recombination at the interface between the perovskite and FTO or HTM.

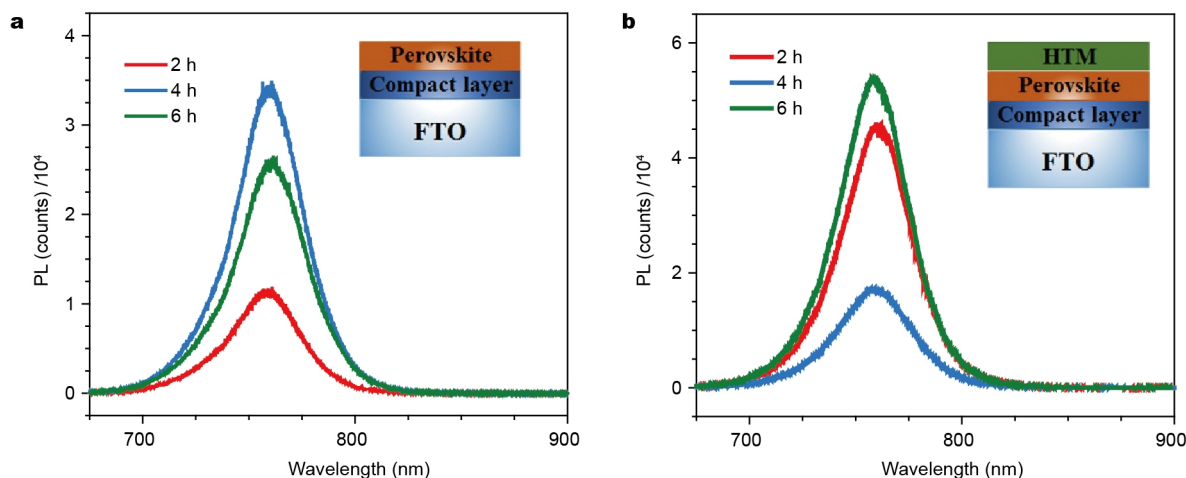


Figure 7 (a) PL of FTO/TiO₂ compact layer from sols aged for different period of time/perovskite film without charge separation and (b) PL of FTO/TiO₂ compact layer/perovskite/HTM with charge separation: excited electrons injected to the TiO₂ layer while holes injected to the HTM. The insets show the structures of the samples.

The J - V curves of the solar cells constructed with different compact TiO_2 layers corroborate the results and explanations presented above. The TiO_2 compact film made by the sol aged for 4 h can effectively reduce charge recombination and increase light absorption in perovskite film, which would enhance the J_{sc} and the open circuit voltage (V_{oc}) of the solar cells. The FF is another importance parameter of the solar cells which generally represents how “difficult” or how “easy” the photo-generated carriers can be extracted out of a photovoltaic device. As shown in Fig. 8 and Table 2, the devices with TiO_2 compact layers made by spin coating the sol aged for 0, 2, to 4 h show a significant enhancement in J_{sc} from 14.75 to 20.45 mA cm^{-2} and a slight increase in FF from 0.68 to 0.74. Consequently, the PCE increases from 10.16% to 15.66%. For the solar cells constructed on the compact layers made from the sols aged for 6 and 8 h, the J_{sc} and FF decrease from 20.45 to 9.01 mA cm^{-2} and 0.74 to 0.63, most likely due to the excessive transport resistance through the thick films and the charge recombination through the cracks [38]. The best PCE of 15.66% was obtained when the compact layer was made from 4 h aged sol, and an average efficiency of 14.01% in 20 samples was achieved. The solar cells with compact layers made from the sols aged less than 4 h or more than 4 h exhibit lower PCE. Such a variation in PCE is consistent and in good agreement with the electrochemical and optical measurements. The CVs and impedance spectra show that the compact films used sol aged for 4 h have better hole blocking effect and, thus, more reduction in charge recombination, therefore, the J_{sc} and FF of the corresponding cells would be improved. In addition, the PL demonstrates that the compact film made from 4 h aged sol with large roughness likely results in the deposition of thick perovskite film for more efficient light absorption and facilitates better charge injection. It should also be noted that the present study revealed no appreciable impact of TiO_2 compact layers made from sols aged for a different duration on the J - V hysteresis commonly observed in perovskite solar cells as shown in

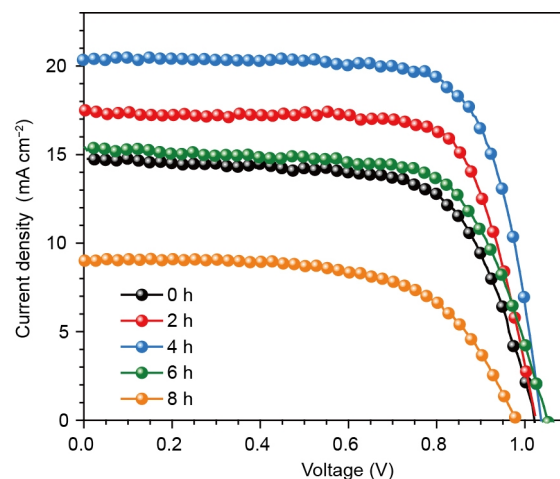


Figure 8 The J - V curves of the perovskite solar cells with TiO_2 compact layers made from sols aged for different duration: 0, 2, 4, 6 and 8 h.

Fig. S4.

CONCLUSIONS

The present work demonstrated and reaffirmed that the performance of perovskite solar cells can be affected by many subtle variation in materials, processing conditions and fabrication procedure. When a compact TiO_2 thin film is made from the same sol but with a varied duration of aging time, the PCE of the perovskite solar cells varied significantly. It was found that the coverage, surface morphology, and thickness of the compact layer strongly affect the performance of the solar cells. The compact film made from sol aged for 4 h possesses the largest roughness and full coverage with moderate film thickness offering the deposition of thick perovskite film with presumably a good adhesion, effective light scattering, good charge injection and separation, and collectively leads to the best PCE of 15.66%, more than 50% improvement from the solar cell based on TiO_2 films made from sols aged less or more than 4 h.

Table 2 Performances of the perovskite solar cells with TiO_2 compact layers deposited by spin coating sol which aged for 0, 2, 4, 6 and 8 h, respectively

Devices	V_{oc} (V)	J_{sc} (mA cm^{-2})	FF	PCE (%)
0 h	1.017	14.75	0.68	10.16
2 h	1.023	17.49	0.73	13.18
4 h	1.031	20.45	0.74	15.66
4 h ^{a)}	1.014	19.04	0.73	14.01
6 h	1.048	15.39	0.68	11.03
8 h	0.978	9.01	0.63	5.56

a) The average values of 20 cells fabricated with the 4 h aged TiO_2 precursor.

Received 14 July 2016; accepted 17 August 2016;
published online 1 September 2016

- Chen X, Mao SS. Titanium dioxide nanomaterials: synthesis, properties, modifications, and applications. *Chem Rev*, 2007, 107: 2891–2959
- Yang HG, Liu G, Qiao SZ, *et al.* Solvothermal synthesis and photoreactivity of anatase TiO₂ nanosheets with dominant {001} facets. *J Am Chem Soc*, 2009, 131: 4078–4083
- Kojima A, Teshima K, Shirai Y, *et al.* Organometal halide perovskites as visible-light sensitizers for photovoltaic cells. *J Am Chem Soc*, 2009, 131: 6050–6051
- Sunada K, Kikuchi Y, Hashimoto K, *et al.* Bactericidal and detoxification effects of TiO₂ thin film photocatalysts. *Environ Sci Technol*, 1998, 32: 726–728
- Zhang J, Li S, Yang P, *et al.* Deposition of transparent TiO₂ nanotubes-films via electrophoretic technique for photovoltaic applications. *Sci China Mater*, 2015, 58: 785–790
- Yoo B, Kim KJ, Bang SY, *et al.* Chemically deposited blocking layers on FTO substrates: effect of precursor concentration on photovoltaic performance of dye-sensitized solar cells. *J Electroanal Chem*, 2010, 638: 161–166
- Dar MI, Ramos FJ, Xue Z, *et al.* Photoanode based on (001)-oriented anatase nanoplatelets for organic–inorganic lead iodide perovskite solar cell. *Chem Mater*, 2014, 26: 4675–4678
- Tian J, Gao R, Zhang Q, *et al.* Enhanced performance of CdS/CdSe quantum dot cosensitized solar cells via homogeneous distribution of quantum dots in TiO₂ film. *J Phys Chem C*, 2012, 116: 18655–18662
- McGehee MD. Perovskite solar cells: continuing to soar. *Nat Mater*, 2014, 13: 845–846
- Grätzel M. The light and shade of perovskite solar cells. *Nat Mater*, 2014, 13: 838–842
- Hodes G. Perovskite-based solar cells. *Science*, 2013, 342: 317–318
- Zheng K, Zhu Q, Abdellah M, *et al.* Exciton binding energy and the nature of emissive states in organometal halide perovskites. *J Phys Chem Lett*, 2015, 6: 2969–2975
- Wang Q, Chen H, Liu G, *et al.* Control of organic–inorganic halide perovskites in solid-state solar cells: a perspective. *Sci Bull*, 2015, 60: 405–418
- Liu D, Kelly TL. Perovskite solar cells with a planar heterojunction structure prepared using room-temperature solution processing techniques. *Nat Photon*, 2013, 8: 133–138
- Sung SD, Ojha DP, You JS, *et al.* 50 nm sized spherical TiO₂ nanocrystals for highly efficient mesoscopic perovskite solar cells. *Nanoscale*, 2015, 7: 8898–8906
- Ip AH, Quan LN, Adachi MM, *et al.* A two-step route to planar perovskite cells exhibiting reduced hysteresis. *Appl Phys Lett*, 2015, 106: 143902
- Ball JM, Lee MM, Hey A, *et al.* Low-temperature processed meso-structured to thin-film perovskite solar cells. *Energy Environ Sci*, 2013, 6: 1739–1743
- Liu M, Johnston MB, Snaith HJ. Efficient planar heterojunction perovskite solar cells by vapour deposition. *Nature*, 2013, 501: 395–398
- Peng B, Jungmann G, Jäger C, *et al.* Systematic investigation of the role of compact TiO₂ layer in solid state dye-sensitized TiO₂ solar cells. *Coordin Chem Rev*, 2004, 248: 1479–1489
- Kavan L, Tétreault N, Moehl T, *et al.* Electrochemical characterization of TiO₂ blocking layers for dye-sensitized solar cells. *J Phys Chem C*, 2014, 118: 16408–16418
- Liang Z, Zhang Q, Wiranwetchayan O, *et al.* Effects of the morphology of a ZnO buffer layer on the photovoltaic performance of inverted polymer solar cells. *Adv Funct Mater*, 2012, 22: 2194–2201
- Gao Q, Yang S, Lei L, *et al.* An effective TiO₂ blocking layer for perovskite solar cells with enhanced performance. *Chem Lett*, 2015, 44: 624–626
- Cojocaru L, Uchida S, Sanehira Y, *et al.* Surface treatment of the compact TiO₂ layer for efficient planar heterojunction perovskite solar cells. *Chem Lett*, 2015, 44: 674–676
- Eperon GE, Burlakov VM, Docampo P, *et al.* Morphological control for high performance, solution-processed planar heterojunction perovskite solar cells. *Adv Funct Mater*, 2014, 24: 151–157
- Jeon NJ, Noh JH, Kim YC, *et al.* Solvent engineering for high-performance inorganic-organic hybrid perovskite solar cells. *Nat Mater*, 2014, 13: 897–903
- Aharon S, Gamliel S, Cohen BE, *et al.* Depletion region effect of highly efficient hole conductor free CH₃NH₃PbI₃ perovskite solar cells. *Phys Chem Chem Phys*, 2014, 16: 10512–10518
- Zhao Y, Zhu K. CH₃NH₃Cl-assisted one-step solution growth of CH₃NH₃PbI₃: structure, charge-carrier dynamics, and photovoltaic properties of perovskite solar cells. *J Phys Chem C*, 2014, 118: 9412–9418
- Hench LL, West JK. The sol-gel process. *Chem Rev*, 1990, 90: 33–72
- Brinker CJ, Scherer GW. *Sol-Gel Science: the Physics and Chemistry of Sol-Gel Processing*. New York: Academic Press, 1990
- Tian J, Zhang Q, Zhang L, *et al.* ZnO/TiO₂ nanocable structured photoelectrodes for CdS/CdSe quantum dot co-sensitized solar cells. *Nanoscale*, 2013, 5: 936–943
- Moehl T, Im JH, Lee YH, *et al.* Strong photocurrent amplification in perovskite solar cells with a porous TiO₂ blocking layer under reverse bias. *J Phys Chem Lett*, 2014, 5: 3931–3936
- Liu D, Yang J, Kelly TL. Compact layer free perovskite solar cells with 13.5% efficiency. *J Am Chem Soc*, 2014, 136: 17116–17122
- Xu X, Zhang H, Shi J, *et al.* Highly efficient planar perovskite solar cells with a TiO₂/ZnO electron transport bilayer. *J Mater Chem A*, 2015, 3: 19288–19293
- Zhu L, Shi J, Li D, *et al.* Effect of mesoporous TiO₂ layer thickness on the cell performance of perovskite solar cells. *Acta Chim Sin*, 2015, 73: 261
- Dualeh A, Moehl T, Tétreault N, *et al.* Impedance spectroscopic analysis of lead iodide perovskite-sensitized solid-state solar cells. *ACS Nano*, 2014, 8: 362–373
- Fei C, Guo L, Li B, *et al.* Controlled growth of textured perovskite films towards high performance solar cells. *Nano Energy*, 2016, 27: 17–26
- Pascoe AR, Yang M, Kopidakis N, *et al.* Planar versus mesoscopic perovskite microstructures: the influence of CH₃NH₃PbI₃ morphology on charge transport and recombination dynamics. *Nano Energy*, 2016, 22: 439–452
- Zhao Z, Chen X, Wu H, *et al.* Probing the photovoltage and photocurrent in perovskite solar cells with nanoscale resolution. *Adv Funct Mater*, 2016, 26: 3048–3058

Acknowledgments This work was supported by the “Thousands Talents” program for pioneer researcher and his innovation team, China, and the National Natural Science Foundation of China (51374029 and 91433102), the Program for New Century Excellent Talents in the University (NCET-13-0668), and the Fundamental Research Funds for the Central Universities (FRF-TP-14-008C1).

Author contributions Guo L, Fei C, Zhang R, Li B and Shen T performed the fabrication of the devices, materials synthesis, characterization and photoelectrochemical measurements. Guo L involved in analysis and discussion, and wrote the manuscript. Tian J and Cao G proposed the strategy, supervised the design of experiments and revised the manuscript.

Conflict of interest The authors declare that they have no conflict of interest.

Supplementary information Supplementary data are available in the online version of this paper.



Lixue Guo is currently a master candidate in Beijing Institute of Nanoenergy and Nanosystems, Chinese Academy of Sciences. Her research interest focuses on the application of plasmon effect in perovskite solar cells.



Jianjun Tian is a professor at the Advanced Material and Technology Institute, University of Science and Technology Beijing. He has worked as a visiting scholar at the University of Washington in 2011. His current research is focused on the fabrication of high quality quantum dot sensitized solar cells and perovskite solar cells.



Guozhong Cao is a Boeing-Steiner Professor of materials science and engineering at the University of Washington, and a senior professor at Beijing Institute of Nanoenergy and Nanosystems, Chinese Academy of Sciences. He has published more than 500 papers, 8 books and 4 proceedings. His recent research is focused mainly on solar cells, lithium-ion batteries, super capacitors, and hydrogen storage.

胶体陈化时间对TiO₂致密层及钙钛矿太阳能电池性能的影响探究

郭立雪¹, 费成斌¹, 张荣¹, 李波², 沈婷², 田建军^{1,2*}, 曹国忠^{1,3*}

摘要 钙钛矿太阳能电池的光伏性能有赖于对材料的化学组分、晶体以及微观结构的精细调控和对工艺条件和制备过程的控制. 本工作针对不同陈化时间的溶胶制备的TiO₂致密层与太阳能电池性能之间的关联性进行了研究. 研究中, 通过溶胶-凝胶法制备了致密、均匀的TiO₂薄膜, 并研究了其表面形貌及厚度对钙钛矿太阳能电池性能的影响. 通过调节溶胶的陈化时间可以实现对TiO₂表面形貌和厚度的控制, 由于陈化后的溶胶会提高TiO₂致密层的覆盖度, 粗糙度及光的折射率, 并有效阻挡电子的复合, 从而导致钙钛矿太阳能电池中短路电流密度和填充因子提升. 钙钛矿薄膜的吸收光谱, 光致发光谱, TiO₂薄膜的循环伏安测试及整个电池的交流阻抗谱的测试结果, 也进一步论证了该结论. 结果显示使用陈化时间为4 h的溶胶制备的钙钛矿电池获得了15.7%的能量转化效率, 比使用0 h陈化的溶胶制备的太阳能电池效率高50%, 是使用陈化时间为8 h的溶胶制备的太阳能电池效率的3倍.